

# Hartree-Fock theory of a current-carrying electron gas

H. Mera,<sup>1,2</sup> P. Bokes,<sup>1,3</sup> and R.W. Godby<sup>1</sup>

<sup>1</sup>*Department of Physics, University of York,  
Heslington, York YO10 5DD, United Kingdom.*

<sup>2</sup>*Niels Bohr Institute and Nano-Science Center,  
Universitetsparken 5, DK-2100 Copenhagen .*

<sup>3</sup>*Department of Physics, Faculty of Electrical Engineering and Information Technology,  
Slovak University of Technology, Ilkovičova 3, 812 19 Bratislava, Slovakia.*

(Dated: May 5, 2019)

## Abstract

State-of-the-art simulation tools for non-equilibrium quantum transport systems typically take the current-carrier occupations to be described in terms of equilibrium distribution functions characterised by two different electro-chemical potentials, while for the description of electronic exchange and correlation, the local density approximation (LDA) to density functional theory (DFT) is generally used. However this involves an inconsistency because the LDA is based on the homogeneous electron gas *in equilibrium*, while the system is not in equilibrium and may be far from it. In this paper we analyze this inconsistency by studying the interplay between non-equilibrium occupancies obtained from a maximum entropy approach and the Hartree-Fock exchange energy, single-particle spectrum and exchange hole, for the case of a two-dimensional homogeneous electron gas. The current-dependence of the local exchange potential is also discussed. It is found that the single-particle spectrum and exchange hole have a significant dependence on the current which has not been taken into account in practical calculations. The exchange energy and the local exchange potential, however, are shown to change very little with respect to their equilibrium counterparts. The weak dependence of these quantities on the current is explained in terms of the symmetries of the exchange hole.

PACS numbers: 71.10.-w, 71.10.Ca, 71.70.Gm, 73.23.-b

## I. INTRODUCTION

One of the uncontrollable approximations introduced in *ab initio* calculations of the transport properties of nano-scale conductors consists in the application of DFT, a ground state theory, outside the equilibrium regime. An immediate consequence of this approximation is that these properties are typically calculated at the level of the LDA, which is derived from the case of a homogeneous electron gas in equilibrium. The extent to which these approximations might affect the calculated electronic structure of the non-equilibrium systems remains largely unknown and thus a comparison between electronic properties calculated *exactly* for an admittedly highly idealised non-equilibrium system and those of the same system in equilibrium constitutes a particularly simple way of approaching and illustrating this problem.

In order to put these ideas into practice we will consider a two-dimensional electron gas in equilibrium and in a *model* non-equilibrium state. To model a homogeneous electron gas outside equilibrium we will assume that the non-equilibrium steady-state of the two dimensional electron gas can be characterized by the average total energy of the electron gas and by *different* average numbers of left- and right-moving electrons and that the non-equilibrium steady-state is given by the density matrix that maximises the entropy of the electron gas with constraints on the above mentioned averages.

Such an assumption leads in the non-interacting case to a momentum distribution characterized by *two Fermi hemispheres of different radii*; we take a pragmatic approach here and ignore the problems associated with the discontinuous character of this momentum distribution for the time being since we are interested in the question of how these current-inducing constraints affect the electronic properties of the two dimensional electron gas. Note that this type of momentum distribution is precisely of the form used in Landauer-Büttiker-type of approaches and thus familiar to the *ab initio* quantum transport community<sup>1,2,3,4</sup> which constantly makes use of it. Similar momentum distributions are predicted by semi-classical transport theories in two dimensional quantum point contacts<sup>5</sup>. Alternatively, and perhaps also more physically, a current-constraint may be used instead of the above-mentioned constraint to search for the non-equilibrium maximum entropy density matrix<sup>6,7,8,9</sup>.

To summarise, we will maximize the entropy of a two-dimensional homogeneous electron gas with constraints on the average numbers of left- and right-moving electrons to obtain

a description of a steady-state at the Hartree-Fock level of approximation, which can then be used to obtain the electronic structure of the gas in the presence of a current and to compare it with the usual approximations. The rest of the paper is organized as follows: in the next section we discuss our theoretical approach to the problem and its numerical implementation; in Section III we discuss the current-dependence of the Hartree-Fock pair probability distribution, single particle spectrum, total energy and local exchange potential. We conclude with a discussion of the relevance of our work for practical calculations.

## II. THEORY

In order to proceed let us consider the entropy per unit area of the two dimensional electron gas to be a functional of the electronic occupancies given by<sup>10</sup>:

$$S[f(\mathbf{k})] = - \int_{\mathfrak{R}^2} \frac{d^2\mathbf{k}}{2\pi^2} [f(\mathbf{k}) \ln f(\mathbf{k}) + (1 - f(\mathbf{k})) \ln (1 - f(\mathbf{k}))]. \quad (1)$$

The electronic occupancies are written as:

$$f(\mathbf{k}) = \begin{cases} f_L(\mathbf{k}) & \text{if } k_x < 0 \\ f_R(\mathbf{k}) & \text{if } k_x > 0 \end{cases}$$

where  $\mathbf{k} = (k_x, k_y)$  and  $f_{L/R}$  are the occupation functions to be varied independently in order to maximise Eq. (1) with constraints on the average total energy per unit area and different average numbers of left- and right-going particles per unit area. In the finite-temperature Hartree-Fock approximation the average total energy is given by:

$$\langle E \rangle = 2 \int_{\mathfrak{R}^2} \frac{d^2\mathbf{k}}{(2\pi)^2} f(\mathbf{k}) \frac{k^2}{2} - \int_{\mathfrak{R}^2} \frac{d^2\mathbf{k}'}{(2\pi)^2} \int_{\mathfrak{R}^2} \frac{d^2\mathbf{k}}{(2\pi)^2} f(\mathbf{k}) f(\mathbf{k}') v(\mathbf{k}, \mathbf{k}') \quad (2)$$

where  $v(\mathbf{k}, \mathbf{k}') = 2\pi/|\mathbf{k} - \mathbf{k}'|$  is the Fourier transform of the Coulomb interaction in two dimensions. The number of left- and right-going electrons per unit area can be written as:

$$n_{L(R)} = \frac{2}{(2\pi)^2} \int_{k_x < (>) 0} d^2\mathbf{k} f_{L(R)}(\mathbf{k}) \quad (3)$$

In order to maximise the entropy functional with respect to  $f_{L/R}$  subject to the above-mentioned constraints we use the method of Lagrange multipliers and consider the auxiliary functional

$$\mathcal{L}[f(\mathbf{k})] = S - \beta (\langle E \rangle - \mu_L n_L - \mu_R n_R), \quad (4)$$

together with the extremal condition

$$\frac{\delta \mathcal{L}}{\delta f_{L/R}} = 0. \quad (5)$$

A straightforward calculation shows that the occupation functions that maximise the entropy functional with constraints in the above-mentioned averages are given by:

$$f_{L,R}(\mathbf{k}) = \frac{1}{1 + \exp[\beta(k^2/2 + \epsilon_x(\mathbf{k}) - \mu_{L,R})]} \quad (6)$$

where

$$\epsilon_x(\mathbf{k}) = -\frac{1}{(2\pi)^2} \left( \int_{k_x < 0} d^2\mathbf{k}' f_L(\mathbf{k}') v(\mathbf{k}, \mathbf{k}') + \int_{k_x > 0} d^2\mathbf{k}' f_R(\mathbf{k}') v(\mathbf{k}, \mathbf{k}') \right) \quad (7)$$

i.e., the occupations that maximise the entropy are similar to the ones of the Landauer-Büttiker approach but with a modified exchange part of the spectrum. In the calculation we fix the ratio  $n_L/n_R$ , that together with the charge neutrality condition  $n_L + n_R = 1/(\pi r_s^2)$  completely determines both  $n_L$  and  $n_R$ . With the equilibrium spectrum as a trial  $\epsilon_x(\mathbf{k})$  we solve Eqs. (3) for  $\mu_L$  and  $\mu_R$ . With these values of  $\mu_{L,R}$  a new spectrum is constructed using Eq. (7) and the iteration is completed and subsequently repeated until the input and output spectra are identical to each other within the desired tolerance. All the results presented here are obtained in the  $\beta \rightarrow \infty$ -limit, where our approach is equivalent to that of Hershfield<sup>11</sup> in the Hartree-Fock approximation<sup>14</sup>. Once the self-consistent spectrum and occupation factors are obtained, other quantities like the exchange-energy and exchange hole can be easily obtained. From these we can study how the local exchange potential of the electron gas depends on the current density<sup>15</sup>.

### III. RESULTS

#### A. Hartree-Fock pair distribution function

Let us begin by discussing the current dependence of the Hartree-Fock pair distribution function for spin-like electrons, which is given by:

$$g(\mathbf{r}, \mathbf{r}') = 1 - \left| \frac{1}{n} \int \frac{d^2\mathbf{k}}{(2\pi)^2} \exp[-i\mathbf{k} \cdot (\mathbf{r} - \mathbf{r}')] f(\mathbf{k}) \right|^2 \quad (8)$$

and shown for  $n_L/n_R = 0.5$  in Figure 1-(a). For  $n_L = n_R$ ,  $g$  is spherically symmetric while for  $n_L \neq n_R$  is elongated in the direction of the current. Similar phenomenology has been

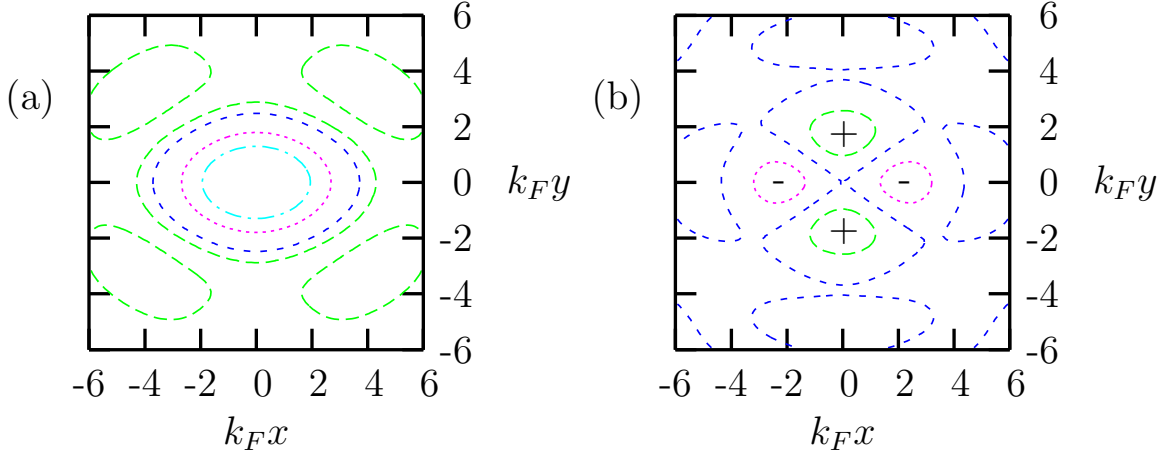


FIG. 1: (Color online). (a) Pair distribution function for like spins in the non-equilibrium regime ( $n_L/n_R = 0.5$ ). In the non-equilibrium regime the exchange-hole is elongated along the direction of the current. The contours are at  $g = 0.5, 0.75, 0.9$  and  $0.95$ . (b) Difference between the equilibrium and non-equilibrium holes,  $\Delta g$  (see text). The contours are drawn at  $0.1$  (dashed),  $-0.1$  (dotted) and  $0$  (dotted).  $\Delta g$  is oscillating, integrates to zero and has a marked antisymmetric character. Thus the current dependence of the local exchange potential and exchange energy is expected to be weak.

reported previously by Skudlarski and Vignale for the three dimensional electron gas in the presence of a magnetic field<sup>12</sup>, where the exchange hole is elongated in the direction of the field. In Ref. 12 the elongation arises from the change of occupancies associated with the Zeeman splitting due to the externally applied magnetic field. In the present case the elongation of the hole can be understood in terms of the change in the electronic occupancies that result from our constrained maximization of the entropy functional. In both cases the elongation of the hole is the result of the change in the polarizability induced by the change in the occupancies<sup>12</sup>.

Note that the difference between the equilibrium and non-equilibrium exchange holes,  $\Delta g = g_{eq} - g_{neq}$ , shown in Figure 1-(b), has a strong antisymmetric character, i.e., defining  $\mathbf{R} = \mathbf{r} - \mathbf{r}' = (X, Y)$  then  $\Delta g(X, Y) \sim -\Delta g(Y, X)$ . We shall return to this point later in the text when discussing the weak dependence of the exchange energy on the current density.

## B. Single-Particle spectrum

Figure 2 shows the self-consistent single-particle energy spectrum. Fig.2-(a) shows the total (kinetic + exchange) spectrum while in Fig.2-(b) we plotted only its exchange part on the  $k_y = 0$  line as given by Eq. (7) for  $n_L = n_R$  and  $n_L/n_R = 0.5$ .

The combined effect of the constraints and the exchange interaction shifts the spectrum towards higher values of  $k_x$ . Note also that, when compared to the equilibrium spectrum, the minimum of the non-equilibrium spectrum is less negative. Hence we expect the total non-equilibrium exchange energy to increase with respect to the equilibrium one. Note that the constraints alter the total kinetic energy of the system but do not change the kinetic contribution to the single particle spectrum, since this contribution does not depend on the electronic occupancies. Hence the changes in the single particle spectrum are entirely due to the exchange interaction, which raises (lowers) the single particle energy of electrons with  $k_x < 0$  ( $k_x > 0$ ). The anomalous behaviour in the  $k_x = 0$  plane inherited from the discontinuous character of the maximum entropy momentum distribution can be seen clearly in Fig.2-(a), between  $\mu_L$  and  $\mu_R$ .

The interplay between non-equilibrium occupancies and the single-particle spectrum observed here is just a consequence of the orbital dependence of the Fock operator and will also be seen in any practical calculation that combines a non-equilibrium theory such as the Landauer-Büttiker approach or the Keldysh-NEGF formalism, with an *orbital-dependent* description of the interactions between the electrons, such as the Hartree-Fock approximation. We would like to point out that practical implementations of NEGF formalism typically take the electronic structure of the leads to be that of the equilibrium system (see Ref.13 and references therein), and hence the dependence of the single-particle spectrum on the non-equilibrium current (and vice-versa) is commonly ignored. The validity of this approximation is geometry dependent: it works in quantum point contact geometries while it does not in planar electrode geometries at high currents. As a consequence under the “non-interacting equilibrium lead approximation” the distribution of incoming electrons would be current-independent, while, as this example shows<sup>16</sup>, the unavoidable presence of interactions in the leads induces a current dependence in the non-equilibrium occupancies through the exchange part of the single particle spectrum. Unless the geometry is adequately chosen the distribution of incoming electrons will be that of a *non-equilibrium* lead such as ours.

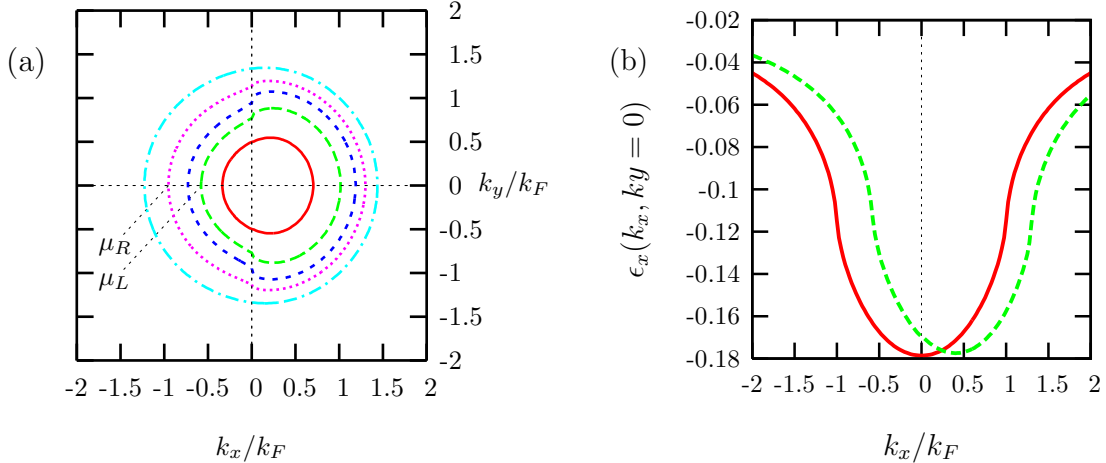


FIG. 2: (Color online). (a) Contour plots of the total single particle energy spectrum of the model non-equilibrium electron gas for  $n_L/n_R = 0.25$  and  $r_s = 4$ . The contours corresponding to  $\mu_L = -1.1 \cdot 10^{-2}$  a.u. and to  $-9.2 \cdot 10^{-2}$  a.u. are labelled. The other contours shown correspond to  $(\mu_L + \mu_R)/2$  (short dashes),  $\mu_L - 0.5 \cdot 10^{-2}$ (a.u.) (solid),  $\mu_R + 0.5 \cdot 10^{-2}$ (a.u.) (dot-dashed). (b) Exchange contribution to the single particle energy spectrum,  $\epsilon_x(\mathbf{k})$ , evaluated on the  $k_y = 0$  line calculated for  $n_L = n_R$  (solid) and  $n_L/n_R = 0.25$  (dashed). The main effect of the non-equilibrium constraints used in our variational approach is to shift the exchange part of the single-particle spectrum towards higher values of  $k_x$ .

### C. Total energy

Once the self-consistent single-particle spectrum is calculated the total exchange energy,  $E_x$ , can be obtained from the second term in the right hand side of Eq. (2). Figure 3 shows the dependence of the  $r_s$ -invariant quantity  $-E_x/E_x^{eq}$  on  $(1 - n_L/n_R)$ . For  $n_L/n_R = 0.25$ , the exchange energy deviates by about 1 – 2% from its equilibrium value. We also see that, even though the non-self-consistent results provide a good estimate to the self-consistent ones, full self-consistency is needed in the non-equilibrium case, even for a homogeneous gas. The error bars in the self-consistent results are estimated by comparing the exact exchange energy in equilibrium with the exchange energy obtained from our code for  $n_L = n_R$  and different values of  $r_s$ . Therefore, the exchange-energy depends on the current-density, but this dependence is extremely weak in our model system. One could now proceed to calculate this current density explicitly and work out a current dependent local density approximation, from the dependence of  $E_x$  on the current density. However, the weak

dependence of the exchange energy on the current density deduced from Fig. 3 means that the current dependence of the local exchange functional is also very weak, and the changes it will induce in the associated LDA-Kohn-Sham effective potential will be well within the error bar of the LDA itself.

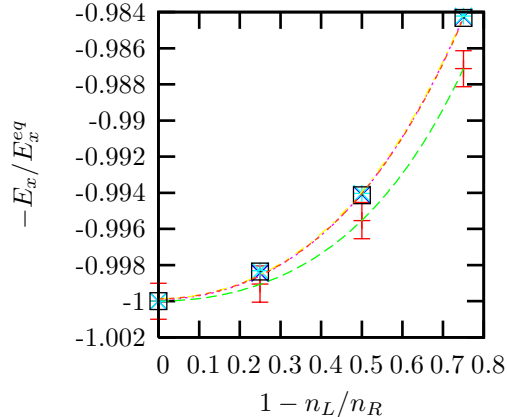


FIG. 3: (Color online). Exchange energy (in units of the equilibrium exchange energy) versus  $1 - n_L/n_R$ . In equilibrium  $1 - n_L/n_R = 0$ . The dashed line shows the self-consistent results with estimated error bars. The non-self-consistent results are also shown with points calculated for different values of  $r_s$  showing that the exchange energy scales with  $r_s$  as  $1/r_s$ . The lines are fits to parabolic functions.

#### D. Local Exchange Potential

The weak dependence of the local exchange potential on the current density can be seen clearly in terms of the symmetries of the exchange hole. Consider the expression for Slater's exchange potential,  $v_x^s$ , in terms of the Hartree-Fock pair distribution function:

$$v_x^s(\mathbf{r}) = \int d^2\mathbf{r}' \frac{[g(\mathbf{r} - \mathbf{r}') - 1]}{|\mathbf{r} - \mathbf{r}'|} n(\mathbf{r}') \quad (9)$$

where  $n(\mathbf{r}')$  is the electron density and  $g(\mathbf{r} - \mathbf{r}')$  is the exchange hole. Then, the difference between equilibrium and non-equilibrium exchange potentials is, for our homogeneous system, given by:

$$\Delta v_x^s = n \int d^2\mathbf{R} \frac{\Delta g(\mathbf{R})}{|\mathbf{R}|} \quad (10)$$

where  $\mathbf{R}$  and  $\Delta g$  are defined as above. From Eq. (10) follows that:

$$\Delta g(X, Y) = -\Delta g(Y, X) \Rightarrow \Delta v_x^s = 0 \quad (11)$$



and hence only the symmetric part of  $\Delta g(X, Y)$  contributes to the deviation of exchange potential with respect to its equilibrium value. Note that  $\Delta g(X, Y)$  is an oscillatory function that integrates to zero which also has a marked antisymmetric character shown in Fig. 1-(b). This explains the weak dependence of  $E_x$  and  $v_x$  on the current-density.

#### IV. CONCLUSIONS

In conclusion we have maximised the entropy of a two-dimensional homogeneous electron gas with constraints on the average total energy and average numbers of left- and right-going electrons to obtain a simplified description of the steady-state within the Hartree-Fock approximation. Our results show that both the single-particle spectrum and the exchange hole depend significantly on the current density while averaged quantities like the local exchange potential or the exchange energy do not.

#### Acknowledgments

The authors gratefully acknowledge useful discussions with J.J. Palacios and J.Fernández-Rossier. We are grateful to Matthieu Verstraete for useful comments on the manuscript. This work was supported by the EU's 6th Framework Programme through the NANOQUANTA Network of Excellence (NMP4-CT-2004-500198), ERG programme of the European Union QuaTraFo (contract MERG-CT-2004-510615), the Slovak grant agency VEGA (project No. 1/2020/05) and the NATO Security Through Science Programme (EAP.RIG.981521).

- 
- <sup>1</sup> S. Datta, *Electronic Transport in Mesoscopic Systems* (Cambridge University Press, 1997).
- <sup>2</sup> H. Haug and A.-P. Jauho, *Quantum Kinetics in Transport and Optics of Semiconductors* (Springer Verlag, 1996).
- <sup>3</sup> J. Taylor, H. Guo, and J. Wang, Phys.Rev. B **63**, 245407 (2001).
- <sup>4</sup> M. Brandbyge et al., Phys. Rev. B **65**, 165401 (2002).
- <sup>5</sup> A. G. M. Jansen, A. P. van Gelder, and P. Wyder, J. Phys. C: Solid St. Phys. **13**, 6073 (1980).
- <sup>6</sup> T. K. Ng, Phys. Rev. Lett. **68**, 1018 (1992).
- <sup>7</sup> O. Heinonen and M. D. Johnson, Phys. Rev. Lett. **71**, 1447 (1993).

- <sup>8</sup> P. Bokes and R. W. Godby, Phys. Rev. B **68**, 125414 (2003).
- <sup>9</sup> P. Bokes, H. Mera, and R. W. Godby, Phys. Rev. B **72**, 165425 (2005).
- <sup>10</sup> T. N. Todorov, J. Hoekstra, and A. P. Sutton, Phil. Mag. B **80**, 421 (2000).
- <sup>11</sup> S. Hershfield, Phys. Rev. Lett. **70**, 2134 (1993).
- <sup>12</sup> P. Skudlarski and G. Vignale, Phys. Rev. B **48**, 8547 (1993).
- <sup>13</sup> H. Mera, P. Bokes, and R. W. Godby, Phys. Rev. B **72**, 085311 (2005).
- <sup>14</sup> i.e., to find the Slater determinant that minimizes the expectation value of the effective Hamiltonian  $\hat{F} = \hat{H}_{HF} - \mu_L \hat{N}_R - \mu_L \hat{N}_R$ .
- <sup>15</sup> For two Fermi-hemispheres of radii  $k_L$  and  $k_R$  the non-interacting electronic current is related to these densities by the expression  $j = \frac{2}{3\sqrt{2\pi}}(n_L + n_R)(n_R^3 - n_L^3)$
- <sup>16</sup> we can see our two-dimensional electron gas as a rough model of one of the leads to which the nanoscale conductor is attached